Research Article

Effect of permanent magnet material on failure-pressure of magnetic fluid seal

Tong Zhang[1] · De-Cai Li[1,2] · Yan-Wen Li[2]

Received: 21 May 2021 / Accepted: 12 July 2021
Published online: 20 July 2021

Abstract
Material properties of permanent magnet in the magnetic fluid seal are important factors that determine the sealing effect. However, the relationship between the magnetic properties of permanent magnet and the failure-pressure has not been studied quantitatively in the available research. In this work, the relationship between material properties of permanent magnet and the failure-pressure of magnetic fluid seal was obtained from theoretical analysis and numerical simulation. The permanent magnet was changed in materials to calculate the failure-pressures of a typical magnetic fluid seal. The results show that the failure pressure of the magnetic fluid seal increases with the increase of the maximum magnetic energy product of the permanent magnet, but there is a turning point. After that, the failure-pressure decreases as the maximum magnetic energy product increases.

Keywords Failure-pressure · Magnetic fluid seal · Maximum magnetic energy product · Permanent magnet · Sintered Nd-Fe-B

1 Introduction

Sealing performances in the aviation field are very strict, and the size of the seal is required to be small enough. As a new sealing method, the magnetic fluid seal has the advantages of zero leakage, long life, and no pollution [1–4]. And it has been widely used in aerospace, medical equipment, chemical machinery, and other fields [5–11]. The sealing principle is that the permanent magnet, pole shoes, and rotation shaft constitute the magnetic circuit, and a magnetic field intensity difference is formed at the sealing gap between the pole teeth and the shaft. Under the action of the magnetic field force, magnetic fluid forms a plurality of O-shaped rings, which can balance the internal and external pressure difference [6, 12]. The failure-pressure of magnetic fluid seal is related to the saturation magnetization of magnetic fluid and the magnetic field gradient of sealing gap. The material properties of the permanent magnet are important factors affecting these two factors. Therefore, it is worthwhile to study the relationship between the failure-pressure of the magnetic fluid seal and the properties of the permanent magnet.

✉ De-Cai Li, lidecai@mail.tsinghua.edu.cn; Tong Zhang, 19121315@bjtu.edu.cn; Yan-Wen Li, lyw19@mails.tsinghua.edu.cn | [1]School of Mechanical, Electronical and Control Engineering, Beijing Jiaotong University, Beijing 100044, China. [2]State Key Laboratory of Tribology, Tsinghua University, Beijing 100084, China.

So far, most studies on permanent magnets have focused on how to improve their performance and future development [13–19]. There is a lack of research on the impact of permanent magnet properties on the failure-pressure of magnetic fluid seal integrally. In publication [20], the influence of sealing gap and centrifugal force on failure-pressure of magnetic fluid seal were studied. Publication [21] studied the effects of the sealing gap, saturation magnetization of magnetic fluid, and the amount of injected magnetic fluid on the failure-pressure of the magnetic fluid seal, but there was no research on permanent magnetic materials scientifically. The material of permanent magnet in publication [12] was told without explanation. In publication [22], the volume of permanent magnet was taken into account. At present, the relationship between material properties of permanent magnet and failure-pressure of the magnetic fluid seal has not been studied completely. In this work, the relationship between the failure-pressure of magnetic fluid seal and the properties of permanent magnetic materials was analyzed in theory and calculated the failure-pressures of the typical magnetic fluid seal with different type of Nd-Fe-B which is commonly used. This research may provide help for the selection of materials in aerospace and other industries.

2 Common permanent magnetic materials

Commonly used permanent magnetic materials can be divided into three categories: first, Al–Ni–Co permanent magnetic materials; Second, permanent magnet ferrites ($BaFe_{12}O_{19}$, $SrFe_{12}O_{19}$); Third, rare earth permanent magnetic materials. The rare earth materials can be divided into three generations: $SmCo_5$, Sm_2Co_{17}, and Nd-Fe-B [23].

Compared with the other types of permanent magnetic material, Nd-Fe-B shows excellent comprehensive magnetic properties. Its magnetic energy product, remanence and coercive force are basically higher than other permanent magnetic materials. Besides, Nd-Fe-B magnets use Fe and Nd which are cheap and rich as raw materials, do not need expensive and scarce rare earth metal Sm and strategic metals Co, Ni and so on, so that the preparation cost is greatly reduced. But its Curie temperature is lower, the temperature stability is poor. It cannot meet the needs of work in high temperature environment. Its main disadvantage is the permissible temperature of around 80 ℃. The world fastest growing market for permanent magnets is for Nd-Fe-B based magnets with high energy product, which would capture 62% market share in 2010 [24].

According to the different production processes, Nd-Fe-B can be divided into the sintered, the bonded, and the hot-pressed. The magnetic properties of sintered Nd-Fe-B are better than those of the bonded and the hot-pressed. Its maximum magnetic energy product, coercive force, and maximum operating temperature are higher than those of the other two kinds. The bonded Nd-Fe-B performance is not as good as the sintered Nd-Fe-B, but it has the advantages of simple process, low cost, small volume, high precision, magnetic field uniformity and stability. The hot-pressed Nd-Fe-B has the advantages of high density, good corrosion resistance and high coercivity. At present, its production costs are high, and the total output is relatively small. Therefore, the sintered Nd-Fe-B is the highest production, the most widely used rare earth permanent magnet material.

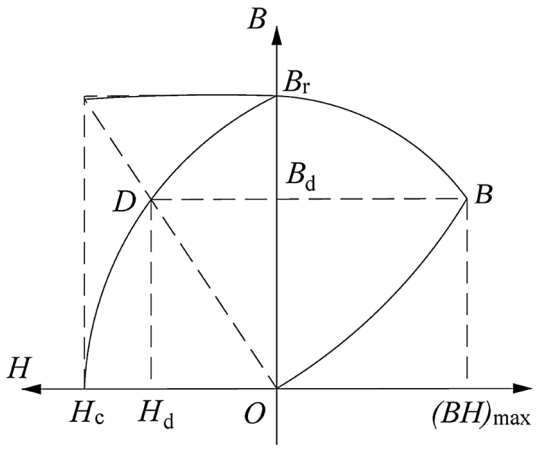

Fig. 1 Demagnetizing curve and energy product curve of magnetic material

Sintered Nd-Fe-B is divided into seven categories according to the intrinsic coercive force [25]. They are N-type, M-type, H-type, SH-type, UH-type, EH-type and TH-type which means that their coercivity is normal, medium, high, superhigh, ultrahigh, extremely high, and tremendous high respectively. Every type has about 7 kinds of sintered Nd-Fe-B. They are different in remanence or coercive force or maximum magnetic energy product. And there are 51 kinds of sintered Nd-Fe-B in total [25]. The permeability for all the types is 1.05.

Figure 1 shows the demagnetization curve and the magnetic energy product curve of permanent magnet materials. Curve B_rDH_c in the second quadrant is the demagnetization curve. The intersection point (B_r) with the longitudinal axis is the remanence, and the intersection point (H_c) with the transverse axis is the coercive force. Curve B_rBO in the first quadrant is the curve of magnetic energy product. The x-coordinate of the point B is the maximum magnetic energy product. The magnetic energy product represents the energy of the magnetic field. The larger the magnetic energy product is, the stronger the

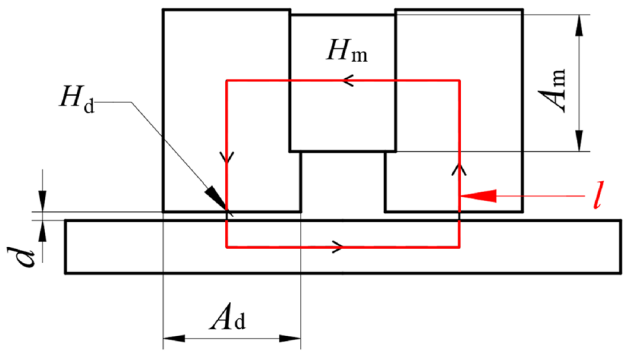

Fig. 2 Magnetic circuit of magnetic fluid seal

magnetic field provided by the permanent magnet is. In addition to the maximum magnetic energy product, magnetic remanence, coercive force, and other factors also affect the failure-pressure of the magnetic fluid seal.

Figure 2 shows a simplified magnetic circuit of the magnetic fluid seal. Assuming that the permanent magnet operates with the maximum magnetic energy product, the magnetic field intensity except the sealing gap is equal to H_m, the magnetic circuit length is $l+2d$, the magnetic field intensity of the sealing gap is H_d and the length of the sealing gap is d. A_m and A_d are the lateral areas of the permanent magnet and the cross-sectional area of the sealing gap respectively.

According to the Ampere Loop Law:

$\Sigma F = H_m l + H_d 2d = 0,,$

$$\rightarrow H_d = -\frac{H_m l}{2d}, \tag{1}$$

where F is the magnetomotive force of the magnetic circuit.

According to the principle of continuity of magnetic flux:

$B_m A_m = B_d A_d,$

$$\rightarrow B_d = \frac{B_m A_m}{A_d}, \tag{2}$$

where B_m is the magnetic flux density of the permanent magnet when it works at the point of the maximum magnetic energy product, B_d is the magnetic flux density of the sealing gap. A_m and A_d are the lateral areas of the permanent magnet and the cross-sectional area of the sealing gap respectively.

Multiply Eq. (1) and Eq. (2) to get

$$H_d B_d = -\frac{H_m B_m l A_m}{2d A_d}, \tag{3}$$

Because $B = \mu_0 H$, Eq. (3) can be written in the following form:

$$B_d^2 = \mu_0 \left(-\frac{H_m B_m l A_m}{2d A_d} \right),$$

$$B_d = \sqrt{-\mu_0 \left(\frac{H_m B_m l A_m}{2d A_d} \right)} = \sqrt{\mu_0 \left(\frac{l A_m}{2d A_d} \right)} \sqrt{-H_m B_m}, \tag{4}$$

When the magnetic fluid seal structure is determined, l, A_m, d, A_d, and μ_0 in Eq. (4) are constants. Therefore, it can be judged that the magnetic induction intensity of the sealing gap (B_d) is proportional to the square-root of maximum magnetic energy product of permanent magnet $(BH)_{max}$. There is a negative sign before H_m because the permanent magnet works at the point of the demagnetization curve which is in the second quadrant. According to the formula for calculating the failure-pressure of magnetic fluid seal $\Delta P = M_s \nabla B$, the failure-pressure is proportional to the square root of the maximum magnetic energy product of the permanent magnet.

3 Numerical simulation method

3.1 Magnetic fluid sealing structure

Fig. 3 shows the magnetic fluid seal used for the numerical simulation. It is a typical structure of magnetic fluid seal which is axisymmetric. The permanent magnet, pole shoes, and shaft form a magnetic circuit, and the magnetic fluid is injected between the pole shoes and shaft. There are 13 pole teeth on every pole shoe. The width of one pole tooth is 2 mm, its height is 7 mm. The clearance between two teeth is 8 mm. And the sealing gap is 1 mm. Besides, the inside diameter of the permanent magnet is 88 mm, the external diameter is 114 mm, and the thickness is 10 mm.

3.2 Numerical simulation method

In this section, the specific simulation process is described. A diester-based magnetic fluid with a density of 1.31 g/cm^3 was used. The magnetic fluid has a maximum magnetization of 15 kA/m. Its permeability is 1. Therefore, magnetic fluid can be regarded as air in the magnetic field simulation. Because the structure is axisymmetric, the magnetic field simulation model was obtained after simplification, as shown in Fig. 4.

Import the simplified model into ANSYS software. First, define the materials as shown in Fig. 5. The materials of pole shoes and shafts are 2Cr13. A1, A2, and A3 represent air, permanent magnet, and 2Cr13 respectively. The permeability of air is 1, and the permeability of 2Cr13 is not

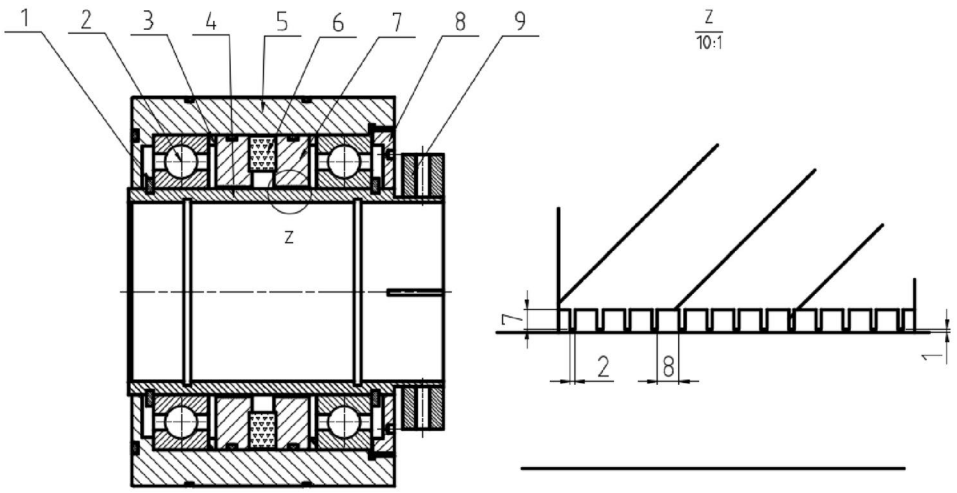

Fig. 3 Magnetic fluid seal: 1-retainer ring, 2-bearing, 3-magnetism-insulator, 4-shaft, 5-shell, 6-magnet, 7-pole shoe 8-threaded end cap, 9-clamping hoop

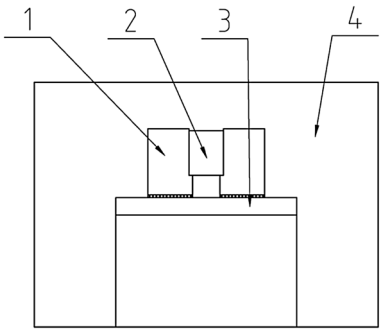

Fig. 4 Magnetic field simulation model of magnetic fluid seal: 1-pole shoe, 2-permanent magnet, 3-shaft, 4-air

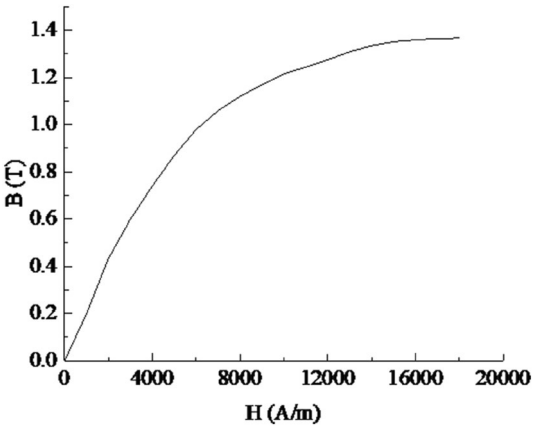

Fig. 6 The magnetization curve of 2Cr13

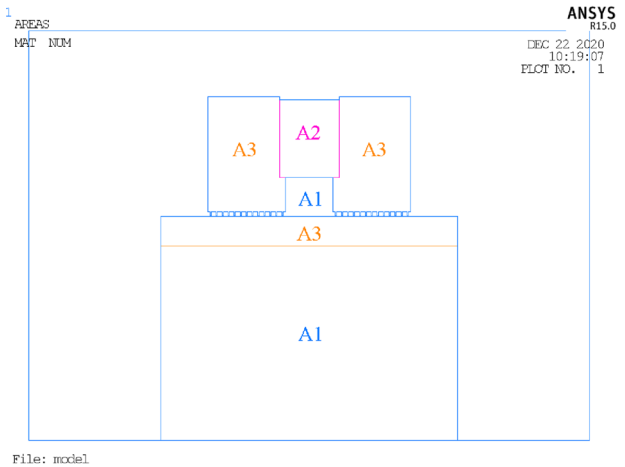

Fig. 5 Material definition for magnetic field simulation of magnetic fluid seal: A1-air, A2-magnetic material, A3-2Cr13

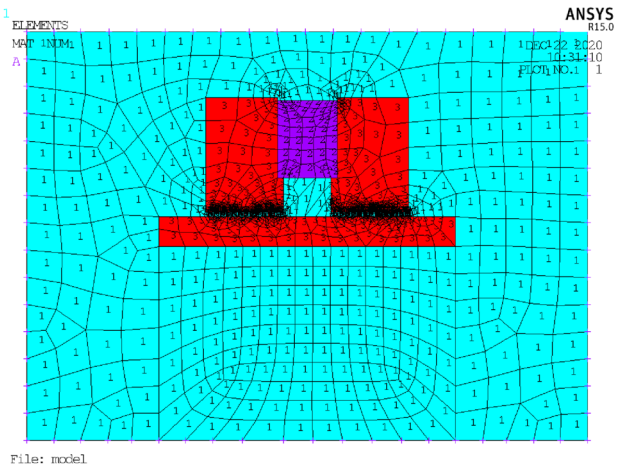

Fig. 7 Meshing and loading of boundary conditions for magnetic field simulation of magnetic fluid seal

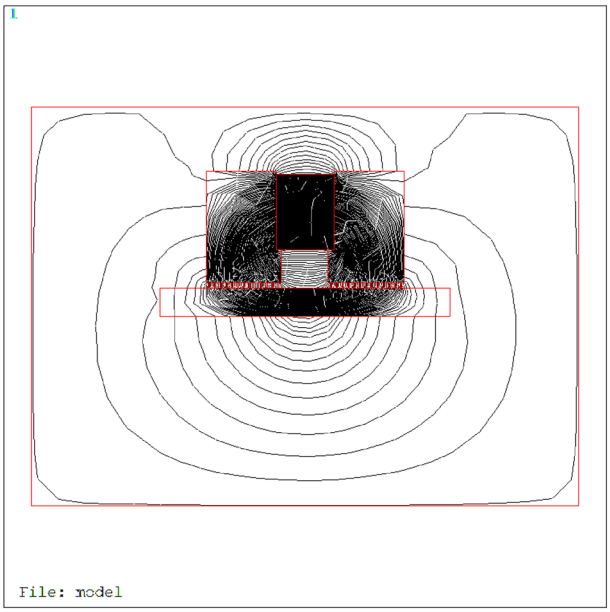

Fig. 8 Magnetic line of force distribution of magnetic fluid seal

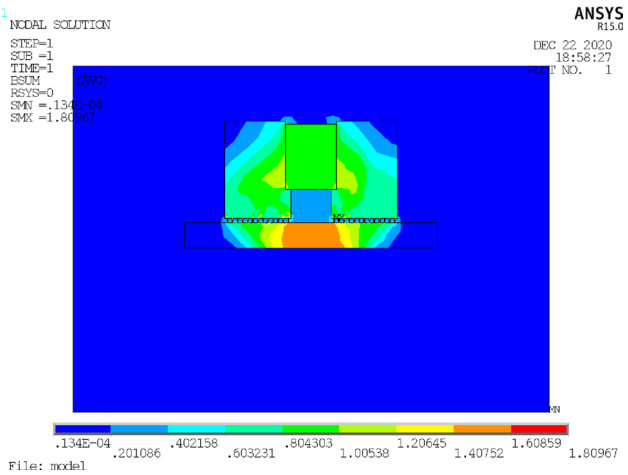

Fig. 9 Magnetic induction intensity cloud map of magnetic fluid seal

constant, so input its magnetization curve as shown in Fig. 6.

The method of intelligent grid partition was adopted, and the level of intelligent grid partition was set to be 4. Figure 7 shows the shape of the generated grid. It can be seen that the grid of the pole teeth is more compact, which is beneficial to analyze the magnetic field intensity at the pole teeth.

Then, a boundary condition was applied, which made the components of magnetic induction intensity equal on the normal line and magnetic field intensity equal on the tangent line. In other words, the magnetic lines of force

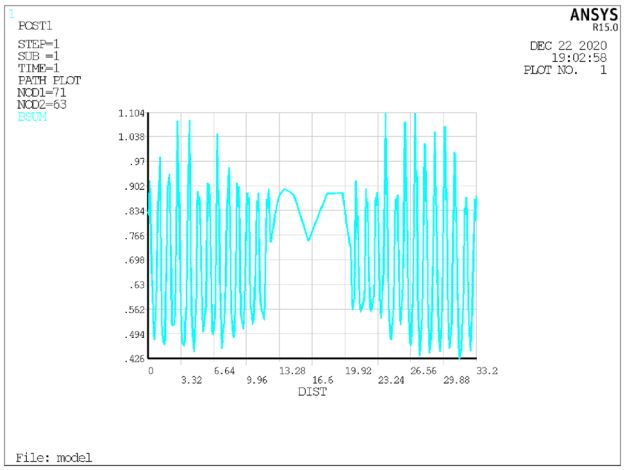

Fig. 10 Magnetic induction intensity on the sealing gap of magnetic fluid seal

were forced to be parallel on the forced boundary to the surface. After the solution, the nephogram of magnetic flux distribution and magnetic induction intensity were obtained, as shown in Figs. 8 and 9.

Define a straight line at the sealing gap, that is, the position of magnetic fluid, and calculate the magnetic induction intensity on the straight line, as shown in Fig. 10. The X coordinate represents the x-coordinate value at the sealing gap, and the y-coordinate represents the corresponding magnetic induction intensity (B). It can be seen from Fig. 10 that the magnetic induction intensity is distributed as waveforms along the x coordinate direction. The parts of the wave crest correspond to the pole teeth in the magnetic fluid seal model. The magnetic induction intensity reaches the maximum in the middle of the pole teeth, and the magnetic induction intensity on both sides of the pole teeth decreases sharply.

MATLAB software can be used to obtain the maximum and minimum magnetic induction intensity of every one-stage pole tooth. And the failure-pressure can be calculated according to the magnetic fluid seal failure-pressure formula

$$\Delta p = \sum \mu_0 \int_{H_{\min}}^{H_{\max}} M dH, \tag{5}$$

$$B = \mu_0 H \tag{6}$$

Table 1 The maximum magnetic energy product of sintered Nd-Fe-B and corresponding average failure-pressure

$(BH)_{max}$/(kJ/m^3)	207	223	247	263	279	287	302
$\overline{p}$/kPa	144.63	144.63	146.28	149.74	150.80	152.01	152.14
$(BH)_{max}$/(kJ/m^3)	318	342	358	374	390	406	
$\overline{p}$/kPa	151.73	151.21	154.37	155.04	153.51	150.51	

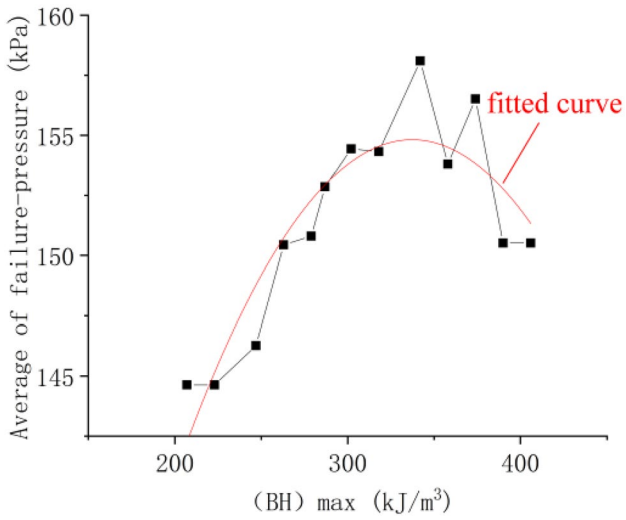

Fig. 11 The maximum magnetic energy product and corresponding average value of failure-pressures

4 Results and discussion

The failure-pressures of the typical magnetic fluid seal introduced in the third section with all the 51 kinds of sintered Nd-Fe-B were calculated. The calculating conditions are the same except for the type of magnet.

The average values of failure-pressures of magnetic fluid seal with the sintered Nd-Fe-B which has the same maximum magnetic energy product are shown in Table 1. Figure 11 shows the relationship between the average value of failure-pressures and maximum magnetic energy product. The smooth curve is a fitting curve.

The fitting curve in Fig. 11 is expressed as

$$Y = 70.68 + 0.50X - 7.39 \times 10^{-4}X^2, \quad (8)$$

where X is the maximum magnetic energy product $(BH)_{max}$. Y is the corresponding average failure-pressure (Δp) of magnetic fluid seal with the sintered Nd-Fe-B which has the same maximum magnetic energy product.

Table 2 The average values of maximum magnetic energy product of each type of sintered Nd-Fe-B and Corresponding failure-pressures

Type	N	M	H	SH	UH	EH	TH
$(BH)_{max}$/(kJ/m^3)	365.22	356.13	337.25	327.43	307	287.71	269.20
ΔP/kPa	147.49	157.90	153.01	150.36	146.87	148.77	146.52

where Δp Failure-pressure of one-stage pole shoe, Pa;μ_0 Vacuum permeability,$\mu_0 = 4\pi \times 10^{-7}$H/m; M Magnetization intensity of magnetic fluid, A/m; H External magnetic field strength, T; B Magnetic inductio intensity, T.

Assuming that the magnetic fluid is saturated. So, the failure-pressure formula can be written as follow:

$$\Delta p = \sum \mu_0 M_s \nabla H = \sum M_s \nabla B \quad (7)$$

where M_s is the saturation magnetization intensity of magnetic fluid.

It can be seen from the fitted curve that the failure-pressure is proportional to the maximum magnetic energy product at first. But there is a maximum value of failure-pressure (155.25 kPa) when the maximum magnetic energy product is 338.29 kJ/m^3. After this point, the failure-pressure decreases as the maximum magnetic energy product increases.

Table 2 shows the average values of maximum magnetic energy product and failure-pressures of the magnetic fluid seal with each type of sintered Nd-Fe-B. Theoretically, magnetic fluid seal with the TH-type sintered Nd-Fe-B which has the lowest average value of maximum magnetic energy product should have the lowest average failure-pressure, and that with the N-type sintered Nd-Fe-B which has the highest average value of maximum magnetic energy product should have the highest average failure-pressure. Whereas, it can be seen from Table 2 that the

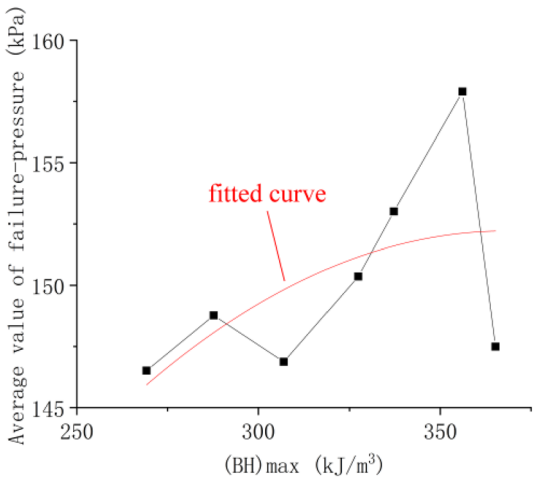

Fig. 12 The average values of the maximum magnetic energy product and failure-pressures

average failure-pressure of M-type is the highest and that of TH-type is the lowest. The reason is that the coercive force of permanent magnet has a certain influence on the failure-pressure of magnetic fluid seal. In a certain range, the greater the coercive force is, the greater the failure-pressure is. Both N-type and M-type have two values of coercive force, and the coercive force of M-type is greater than that of N-type. Nevertheless, other types of sintered Nd-Fe-B have more values of coercive force, so the error is relatively small.

The relationship curve between the average values of maximum magnetic energy product and failure-pressures of magnetic fluid seal with each type of sintered Nd-Fe-B is shown in Fig. 12.

The fitting curve of the average values of the maximum magnetic energy product and failure-pressures in Fig. 12 above is expressed as

$$Y = 64.92 + 0.47X - 6.45 \times 10^{-4}X^2 \quad (9)$$

where X is the average value of maximum magnetic energy product of each type of sintered Nd-Fe-B, Y is the average value of failure-pressures of magnetic fluid seal with each type of sintered Nd-Fe-B.

Also, the failure-pressure of magnetic fluid seal is proportional to the maximum magnetic energy product of the permanent magnet at first. There is a maximum value of failure-pressure (150.54 kPa) when the maximum magnetic energy product is 364.34 kJ/m^3. After this point, the failure-pressure decreases as the maximum magnetic energy product increases.

5 Conclusion

Through analysis in theory and numerical simulation, it was found that the magnetic induction intensity at the sealing gap of the magnetic fluid seal is proportional to the maximum magnetic energy product of the permanent magnet material. And the failure-pressure of magnetic fluid seal is proportional to the maximum magnetic energy product of permanent magnet at first. There is a value of maximum magnetic energy product that makes the failure-pressure largest. Then failure-pressure shows negative relation with the maximum magnetic energy product.

In all types of sintered Nd-Fe-B, magnetic fluid seal with M-type permanent magnet has the highest average failure-pressure, whereas that with TH-type has the lowest average failure-pressure.

Acknowledgements The authors sincerely thanks to Professor Zhi-Li Zhang of Beijing Jiaotong University for her critical discussion and reading during manuscript preparation.

Authors' contributions The author' contributions are as follows: TZ and D-CL was in charge of the whole trial; TZ wrote the manuscript; Y-WL assisted with sampling and laboratory analyses.

Funding Supported by National Natural Science Foundation of China (Grant No. 51735006), National Natural Science Foundation of China (Grant No. 51927810), National Natural Science Foundation of China (Grant No. U1837206) and Beijing Municipal Natural Science Foundation of China (Grant No. 3182013).

Data availability The datasets supporting the conclusions of this article are included within the article.

Declarations

Conflict of interest The authors declare no competing financial interests.

References

1. Odenbach S (2009) Colloidal magnetic fluids: basics, development and application of ferrofluids. Springer, Berlin
2. Mitamura Y, Durst CA (2016) Miniature magnetic fluid seal working in liquid environments. J Magn Magn Mater 431:285–288
3. Yang W, Wang P, Hao R et al (2017) Experimental verification of radial magnetic levitation force on the cylindrical magnets in ferrofluid dampers. J Magn Magn Mater 426:334–339
4. Rosensweig RE (2002) Ferrohydrodynamics. Dover Publications, New York
5. Borbáth T, Bica D, Potencz I, et al. Magnetic nanofluids and magnetic composite fluids in rotating seal systems. Proceedings of the IOP Conference Series: Earth and Environmental Science, Timişoara, Romania, September, 2010: 20–24
6. Matuszewski L, Szydlo Z (2008) The application of magnetic fluids in sealing nodes designed for operation in difficult conditions and in machines used in sea environment. Polish Marit Res 15(3):49–58
7. Mitamura Y, Arioka S, Sakota D et al (2008) Application of a magnetic fluid seal to rotary blood pumps. J Phys: Condens Matter 20(20):204145
8. Chiao J C, De Volder M, Reynaerts D, et al. A ferrofluid seal technology for fluidic microactuators. Proceedings of the Micro- and Nanotechnology: Materials, Processes, Packaging, and Systems III, Adelaide, Australia, December, 2006: 10–13
9. Wal KVD, Ostayen RAJV, Lampaert SGE (2020) Ferrofluid rotary seal with replenishment system for sealing liquids. Tribol Int 150:106372
10. Sreedhar BK, Kumar RN, Sharma P et al (2013) Development of active magnetic bearings and ferrofluid seals toward oil free sodium pumps. Nucl Eng Des 265:1166–1174
11. Cong M, Wen H, Du Y et al (2012) Coaxial twin-shaft magnetic fluid seals applied in vacuum wafer-handling robot. Chin J Mech Eng 25:706–714
12. Chen Y, Li D, Zhang Y et al (2019) Numerical analysis and experimental study on magnetic fluid reciprocating seals. IEEE Trans Magn 55(1):1–6
13. Coey JMD (2011) Hard magnetic materials: a perspective. IEEE Trans Magn 47(12):4671–4681
14. Kaneko Y (2000) Highest performance of Nd-Fe-B magnet over 55 MGOe. IEEE Trans Magn 36(5):3275–3278
15. Vial F, Joly F, Nevalainen E et al (2002) Improvement of coercivity of sintered NdFeB permanent magnets by heat treatment. J Magn Magn Mater 242–245(2):1329–1334
16. Hono K, Sepehri-Amin H (2018) Prospect for HRE-free high coercivity Nd-Fe-B permanent magnets. Scripta Mater 151:6–13
17. Yang Y, Ren RD, Wang YL et al (2020) Effect of Molding pressure on structure and properties of ring-shaped bonded NdFeB magnet. IEEE Trans Magn 56(12):1–5
18. Coey JMD (2019) Perspective and prospects for rare earth permanent magnets. Chin J Eng 6(2):42–68
19. Cui J, Kramer M, Zhou L et al (2018) Current progress and future challenges in rare-earth-free permanent magnets. Acta Mater 158:118–137
20. Zhao M, Zou JB, Hu JH (2006) An analysis on the magnetic fluid seal capacity. J Magn Magn Mater 303(2):e428–e431
21. Gu H, Song PY, Zhu LH et al (2002) The experimenteal study of a magnetic fluid sealing. Chin J Lubr Seal 3:33–35
22. Szczęch M, Horak W (2017) Numerical simulation and experimental validation of the critical pressure value in ferromagnetic fluid seals. IEEE Trans Magn 53(7):1–5
23. Li DC (2010) The theory and application of magnetic fluid seal. Science Press, Beijing (**(in Chinese)**)
24. Gutfleisch O, Willard M, Brück E et al (2011) Magnetic materials and devices for the 21st century: stronger, lighter, and more energy efficient. Adv Mater 23(7):821–842
25. Standardization Administration of China. *Sintered Nd-Fe-B Permanent Magnet Material*, Beijing, China (2017).